SCIENCE CHINA
Life Sciences

• RESEARCH PAPER •

December 2012 Vol.55 No.12: 1082–1091
doi: 10.1007/s11427-012-4414-8

Overexpression of *OsDPR*, a novel rice gene highly expressed under iron deficiency, suppresses plant growth

Naren, ZHANG Peng, MA DengKe, WANG Yi, LI Shuang & YIN LiPing*

College of Life Science, Capital Normal University, Beijing 100048, China

Received July 31, 2012; accepted October 29, 2012

Preliminary microarray analysis of cDNA from rice roots revealed an up-regulated transcript that was highly expressed in a five-day iron deficiency treatment. The entire sequence of this gene was determined by bioinformatics analysis. There were no proteins with significant levels of similarity detected in public databases. This novel gene with unknown biological function was designated as *OsDPR* (dwarf phenotype-related gene). We constructed a stable plant expression vector pCAMBIA1302-*OsDPR*::*GFP* and produced transgenic tobacco plants. The phenotypes suggested that *OsDPR* restrained the growth of transformed plants. To understand the mechanisms of this suppression effect, cell size and number were compared between transformants and wild-type plants. The cell proliferation rate was lower in *OsDPR* transgenic BY-2 cells than in wild-type cells, but *OsDPR* expression did not affect cell size. Moreover, the cell division-related gene *CyclinD2.1*, which is involved in plant growth, was down-regulated in transgenic tobacco plants. These findings suggested that the novel iron-regulated gene *OsDPR* is responsible for the nanism phenotype of transgenic seedlings because of the inhibition of plant cell proliferation.

OsDPR*, iron deficiency, restrained growth, cell division, *CyclinD2.1

Citation: Naren, Zhang P, Ma D K, *et al*. Overexpression of *OsDPR*, a novel rice gene highly expressed under iron deficiency, suppresses plant growth. Sci China Life Sci, 2012, 55: 1082−1091, doi: 10.1007/s11427-012-4414-8

Iron is an essential micronutrient for plants. It functions as an electron donor and acceptor, and it serves as a functional component of a number of metalloenzymes involved in essential biochemical progress such as respiration and photosynthesis [1]. However, excess iron generates hydroxyl radicals, which can damage biological molecules and are not conducive to plant growth [2]. Consequently, maintaining iron homeostasis is crucial for plants. Unfortunately, iron is not easily absorbed because of its low solubility in neutral and alkaline conditions [3]. Thus, the uptake and utilization of iron in plants is highly regulated and coordinated [4].

Higher plants have evolved two iron uptake strategies for iron solubilization and acquisition [5]. Strategy I, the so-called reductive mechanism, functions in dicots and nongraminaceous monocots [6]. First, the roots secrete abundant protons via H^+-ATPases to acidify the rhizosphere under iron deficiency, thereby increasing the solubility of Fe^{3+} [7]. Then, the soil Fe^{3+} is reduced to the more soluble form, Fe^{2+}, by membrane-bound Fe^{3+}-chelate reductases, and then the Fe^{2+} is transported into epidermal cells via the divalent metal transporter (IRT; iron-regulated transporter) [4]. Strategy II is based on chelation, and is specific to graminaceous plants. It is mediated by the synthesis and secretion of natural iron chelators, the mugineic acid (MA) family of phytosiderophores [2]. MAs are secreted from roots and solubilize rhizospheric Fe^{3+} [5]. The resulting Fe^{3+}-MA complexes are absorbed into the root cells by the yellow-stripe-like (YSL) iron transporters [2]. There is evidence that rice acquires iron via strategy I and strategy II [6]. *OsYSL15* and *OsIRT1*, which encode an Fe^{3+}-MA and an Fe^{2+} transporter, respectively, have been characterized in rice [2]. As an efficient Fe^{2+} uptake system, strategy I is

*Corresponding author (email: yinlp@mail.cnu.edu.cn)

activated when the synthesis of deoxygen mugineic acid in strategy II is blocked [8].

Low iron availability causes undesirable changes in plant growth and can be a major abiotic stress in crop production [5]. Thus, investigating the genes that respond to iron deficiency could lead to the production of plants with greater adaptive capacity in iron-deficient environments. In our previous study, we found a wide range of iron-regulated genes in rice roots using a cDNA microarray with 10531 individual sequences [9]. Gene expressions were compared between plants grown in iron-sufficient and iron-deficient conditions for 5 d. In total, 451 cDNA sequences were differentially expressed, among which 203 genes were up-regulated under iron deficiency and 248 genes were down-regulated. Based on bioinformatics and database analyses, we conducted primary functional classification of the genes that were up-regulated under iron deficiency. This current study focuses on *OsDPR* (dwarf phenotype-related gene), one of the genes up-regulated under iron deficiency.

To investigate the function of *OsDPR*, the gene was cloned from rice roots and overexpressed in transgenic tobacco plants. The phenotype showed that the shoots and roots of transformants were shorter than those of wild-type plants, which suggested that *OsDPR* is associated with plant growth regulation. The growth-repression effects of various kinds of factors can be related to the regulation of cell expansion or cell division [10]. In the present study, we examined both the size of cells in transgenic tobacco plants and cell proliferation of transformed BY-2 cells. We concluded that cell proliferation, not cell expansion, was influenced by *OsDPR* overexpression. In addition, the low expression of the cell cycle regulatory gene *CyclinD2.1* in the transformed tobacco plants further indicated that *OsDPR* suppressed plant growth by affecting cell division.

1 Materials and methods

1.1 Bioinformatics analysis of *OsDPR*

NCBI Unigene (http://www.ncbi.nlm.nih.gov/unigene) was used to locate *OsDPR* on the rice chromosome and NCBI Spidey (http://www.ncbi.nlm.nih.gov/IEB/Research/Ostell/Spidey/) was used to analyze the *OsDPR* gene structure. The open reading frame (ORF) of *OsDPR* was predicted and located in the first exon using DNAMAN software. The CpG island was identified by EBI CpGPlot (http://www.ebi.ac.uk/Tools/emboss/cpgplot/). The transmembrane domain was predicted by TMHMM Server v. 2.0 (http://www.cbs.dtu.dk/researchgroups/). The signal peptide was analyzed by SignalP-HMM (euk) (http://www.cbs.dtu.dk/services/SignalP-1.1/). Leucine zipper structures were identified using the ExPASy PROSITE database (http://prosite.expasy.org/). We searched for homologs of OsDPR using protein BLAST (Basic Local Alignment Search Tool) in NCBI.

1.2 Plant materials and growth conditions

Rice seeds (*Oryza sativa* L. cv. *Japonica*) were washed with tap water several times, sterilized with 2% NaClO for 30 min, washed again, and germinated on paper soaked with distilled water at 29°C in the dark for 2–3 d. After germination, the seedlings were transferred to a plate of sterile vermiculite and cultivated in a greenhouse at 25–30°C under a 16/8 h light/dark cycle. When the third leaf appeared, the seedlings were transferred to a plastic container containing distilled water. After 7 d, the seedlings were cultivated on Hoagland nutrient solution either with (100 μmol L^{-1} Fe(II)-EDTA) or without iron treatment for 5 d. Then, the roots were collected from the rice seedlings and used for experiments.

1.3 *OsDPR* ORF cloning and plasmid construction

1.3.1 ORF cloning and determination of transcriptional start site

Total RNA was isolated from rice roots using a NucleoSpin RNA Plant kit (Macherey-Nagle, Germany). RT-PCR was performed according to the manufacturer's protocol (TaKaRa RNA PCR Kit (AMV) Ver. 3.0). The ORF of *OsDPR* was amplified from cDNA using the primers 5′-AGCCATGGATGAGTATAACAGAAATTTTGG-3′ (forward) and 5′-TCACTAGTCTAAAATTTGCTTCTTTCC-TCCT-3′ (reverse). An NcoI site was introduced at the 5′ end of the ORF, and a SpeI site at the 3′ end. The PCR product was purified using the Glassmilk method (Bio-Dev-Tech, China) and subcloned into the pMD-18T vector (TaKaRa, Japan). To determine the transcriptional start site of *OsDPR*, primer set 1 (p1 and p3) and set 2 (p2 and p3) were used to obtain the 5' flanking sequence. We validated the amplification results by sequencing. The sequences of the primers were as follows: p1, 5′-TCATCCAACGCA-TGAGAT-3′; p2, 5′-AGGTCCCAGCTCGGATC-3′; and p3, 5′-CTAAAATTTGCTTCTTTCCTCCT-3′.

1.3.2 Construction of pCAMBIA1302-OsDPR::GFP

We constructed a stable plant expression vector containing *OsDPR*. The coding frame of *OsDPR* was amplified from the plasmid pMD-18T-*OsDPR* using the primers mentioned above and then introduced into the pCAMBIA1302 vector digested with the restriction enzymes *Nco* I and *Spe* I (TaKaRa, Japan) (Figure 1). GFP, as a tag for expression, was linked to the C-terminus of the *OsDPR* ORF. The recombinant plasmid was fully sequenced.

1.4 Transformation of tobacco plants

The stable plant expression vector pCAMBIA1302-*OsDPR::GFP* was transformed into tobacco plants (*Nicotiana tabacum* var. *Samsun NN*) using *Agrobacterium*-mediated transformation. After 2 d of co-cultivation on MS

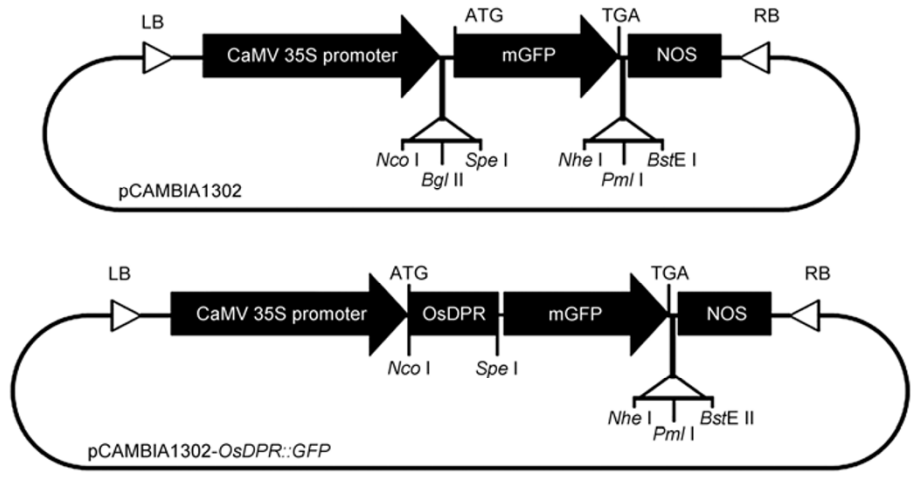

Figure 1 Diagram of the stable expression vectors pCAMBIA1302 and pCAMBIA1302-*OsDPR*::*GFP*.

(Murashige and Skoog) medium in the dark at 28°C, the tobacco leaf discs were transferred to the selection medium (MS medium containing 2.0 mg L^{-1} 6-benzyl aminopurine, 0.5 mg L^{-1} naphthylene acetic acid, 500 mg L^{-1} carbenicillin and 20 mg L^{-1} hygromycin, the selection marker used for transformation) and cultivated at 25–28°C under a 16/8 h light/dark cycle. Shoots 2–3 cm in length were cut and placed on rooting medium (MS medium containing 20 mg L^{-1} hygromycin and 500 mg L^{-1} carbenicillin) for approximately 3 weeks. Some hygromycin-resistant plants developed normal roots on the rooting medium and grew into seedlings after another 2 weeks. We obtained T3 progeny seeds derived from the transformants expressing *OsDPR*. To analyze the phenotype of transgenic tobacco, the plants were cultivated on MS medium without or with iron (37.3 mg L^{-1} Na_2-EDTA, 27.8 mg L^{-1} $FeSO_47H_2O$).

1.5 Observation of tobacco roots and measurement of root cell size

Wild-type and *OsDPR*-transformed tobacco plants were vertically cultured on 1/2 MS medium for 1–2 weeks. The roots were treated with PI (propidium iodide) staining solution (5 μg mL^{-1}) for 5 min and observed under a laser scanning confocal microscope (Leica TCS-SP2, Germany) using a 536 nm excitation wavelength and a 617 nm emission wavelength. Cells in the maturation region of the root tip were chosen for observations and measurements. The length of 120 mature cells was measured from 6 roots of wild-type and *OsDPR*-transformed tobacco plants, respectively. The transgenic plants used for measurements and statistical analysis were from three different lines.

1.6 Transformation of tobacco BY-2 cells

The tobacco BY-2 cells were cultivated in NT medium (MS medium containing 0.6 mg L^{-1} 2,4-dichlorphenoxyacetic acid, pH 5.8) in the dark at 28°C and 120 r min^{-1} for 5 d. *Agrobacterium* strains carrying the vectors were grown in YEB medium to an A_{600} of 0.4–0.5. A 200-μL aliquot of *Agrobacterium* in YEB medium was added with 20 μmol L^{-1} acetosyringone to 8 mL NT medium containing cultivated tobacco BY-2 cells. The cells were placed in the dark at 28°C for 2 d, washed twice with NT medium containing carbenicillin (500 mg L^{-1}), and then centrifuged at 110×*g* for 4 min. The transformed BY-2 cells were selected on 1/2 NT medium containing 500 mg L^{-1} carbenicillin and 20 mg L^{-1} hygromycin as the transformation selection marker.

1.7 Western blotting and GFP detection

Total protein was extracted from wild-type and *OsDPR*-transformed BY-2 cells. A 3-mL aliquot of BY-2 cells was pulverized in liquid nitrogen and suspended in 10 mL extraction buffer (25 mmol L^{-1} Tris-HCl pH 7.5, 10 mmol L^{-1} KCl, 20 mmol L^{-1} $MgCl_2$, 1 mmol L^{-1} DTT, 1 mmol L^{-1} PMSF). After centrifuging at 9200×*g* for 30 min, the supernatant was transferred to a new centrifuge tube, and 6 volumes of 10% TCA were added to the tube. The proteins were precipitated for 2 h at −20°C, and the supernatant was removed after centrifuging at 11100×*g* for 30 min. The pellet was washed with acetone containing 0.07% β-mercaptoethanol for 1 h, centrifuged at 11100×*g* for 30 min, and subjected to two further rounds of washing with ethanol∶ether (1∶1) and centrifugation at 11100×*g* for 30 min. The pellet was dissolved in dissolving solution (62.5 mol L^{-1} Tris-HCl pH 7.5, 2% SDS, 10% glycerol, 5% β-mercaptoethanol, 0.001% bromophenol blue, 4°C). Total proteins were separated by SDS-PAGE [11] and transferred to a PVDF (polyvinylidene difluoride) membrane by electroblotting [12]. An anti-GFP antibody was used for detection.

The GFP tag expressed in *OsDPR* transgenic tobacco plants was detected using a GFP-Meter (Opti-Sciences,

USA) according to the manufacturer's protocol.

1.8 Real-time quantitative PCR and detection of *OsDPR::GFP* expression

Total RNA extraction and RT-PCR were performed as described above. Real-time PCR was performed in a Rotor-Gene 3000 using SYBR Premix Ex Taq (TaKaRa). *OsDPR* was amplified using the primers 5′-TGTGAGCATGGCAATGTATG-3′ (forward) and 5′-AGGTAGCACCAGGTTGATCC-3′ (reverse). The primers for *OsActin*, which was used as the reference gene, were 5′-CAGCACATTCCAGCAGAT-3′ (forward) and 5′-GGCTTAGCATTCTTGGGT-3′ (reverse). The tobacco *CyclinD2.1* gene was amplified using the primers 5′-CACTTAGACAAGGGTAGAG-3′ (forward) and 5′-CCAATAGGACTTTGAGGTA-3′ (reverse). The primers for the reference gene, tobacco *Actin*, were 5′-CTATTCTCCGCTTTGGACTTGGCA-3′ (forward) and 5′-AGGACCTCAGGACAACGGAAACG-3′ (reverse).

The expression of *OsDPR::GFP* was detected by RT-PCR using the primers 5′-GCTTTTCAAGATACCCAGAT-3′ (forward) and 5′-TTACAAACTCAAGAAGGACC-3′ (reverse).

1.9 Subcellular localization of OsDPR

Pieces of onion epidermis were cultivated on MS medium for 1 d at 25°C under a 14/10 h light/dark cycle. *Agrobacterium* strains carrying the vectors were grown in YEB medium to 0.4–0.5 A_{600}, collected by centrifugation, and resuspended in YEB medium. The pieces of onion epidermis were placed in YEB medium containing the *Agrobacteria*, co-cultivated for 40–60 min, and then placed on filter paper to remove excess liquid. Finally, the pieces of onion epidermis were placed in MS medium containing carbenicillin (500 mg L^{-1}) to arrest *Agrobacterium* growth. Two days later, the OsDPR::GFP fusion protein was transiently expressed in the onion epidermal cells, and the fluorescence was observed under a laser scanning confocal microscope (Leica TCS-SP2, Germany) using a 488 nm excitation wavelength and a 505–520 nm emission wavelength to detect GFP.

1.10 Transformation of rice plants

The stable plant expression vector pCAMBIA1302-*OsDPR::GFP* was constructed as described above. The *Agrobacterium*-mediated transformation procedure was as described by Hiei *et al.* (1994).

1.11 Statistical analysis

Data were analyzed using the independent sample *t*-test (SPSS software). A *P*-value less than 0.05 was considered statistically significant. Quantitative results are expressed as mean±standard deviation (SD).

2 Results

2.1 *OsDPR* highly expressed under iron deficiency

The microarray gene expression result of 10531 cDNA sequences indicated that *OsDPR* was one of 203 up-regulated transcripts that were highly expressed in rice roots under a 5-day iron deficiency treatment [9]. To further confirm this result, real-time PCR was used to verify the expression pattern of *OsDPR* in rice. *OsDPR* mRNA was predominantly detected in rice roots on the 5th day of the 5-day iron deficiency treatment (Figure 2), while its expression was negligible under iron-sufficient conditions. The real-time quantitative PCR result was consistent with the results of the cDNA microarray analysis.

2.2 Sequence analysis of *OsDPR*

The EST sequence of *OsDPR* from cDNA microarray analysis was identified in the NCBI EST database. Using *in silico* methods, we obtained a 1.9-kb sequence that was identical to a rice cDNA in NCBI with unknown function. The genome sequence corresponding to the 1.9 kb cDNA was analyzed by bioinformatic methods to determine the entire sequence of *OsDPR*. The sequence of *OsDPR*, which is approximately 3 kb long, is located on chromosome 11, and contains three exons and two introns. A short ORF, which is contained within the first exon, encodes a 9.68-kD protein with 86 amino acids (Figure 3B).

To determine the transcriptional start site (TSS), total RNA was isolated from rice roots and used as a template for RT-PCR. We designed two forward primers, p1 and p2, approximately 20-bp upstream and downstream, respectively, of the predicted TSS. The reverse primer, p3, was designed within the ORF (Figure 3B). In a two-step RT-PCR, 530-bp bands were amplified from rice root total

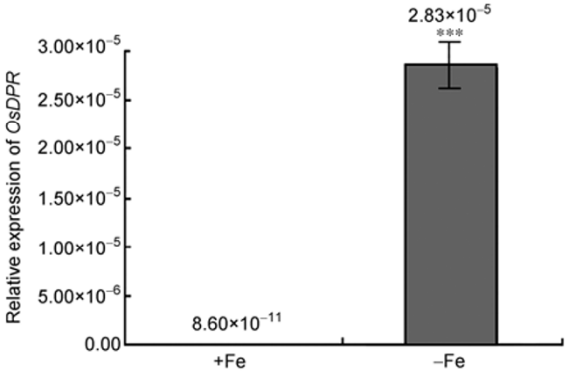

Figure 2 Real-time PCR analysis of *OsDPR* expression in rice roots with (+Fe) or without (–Fe) iron treatment. ***, $P<0.001$, $n=3$.

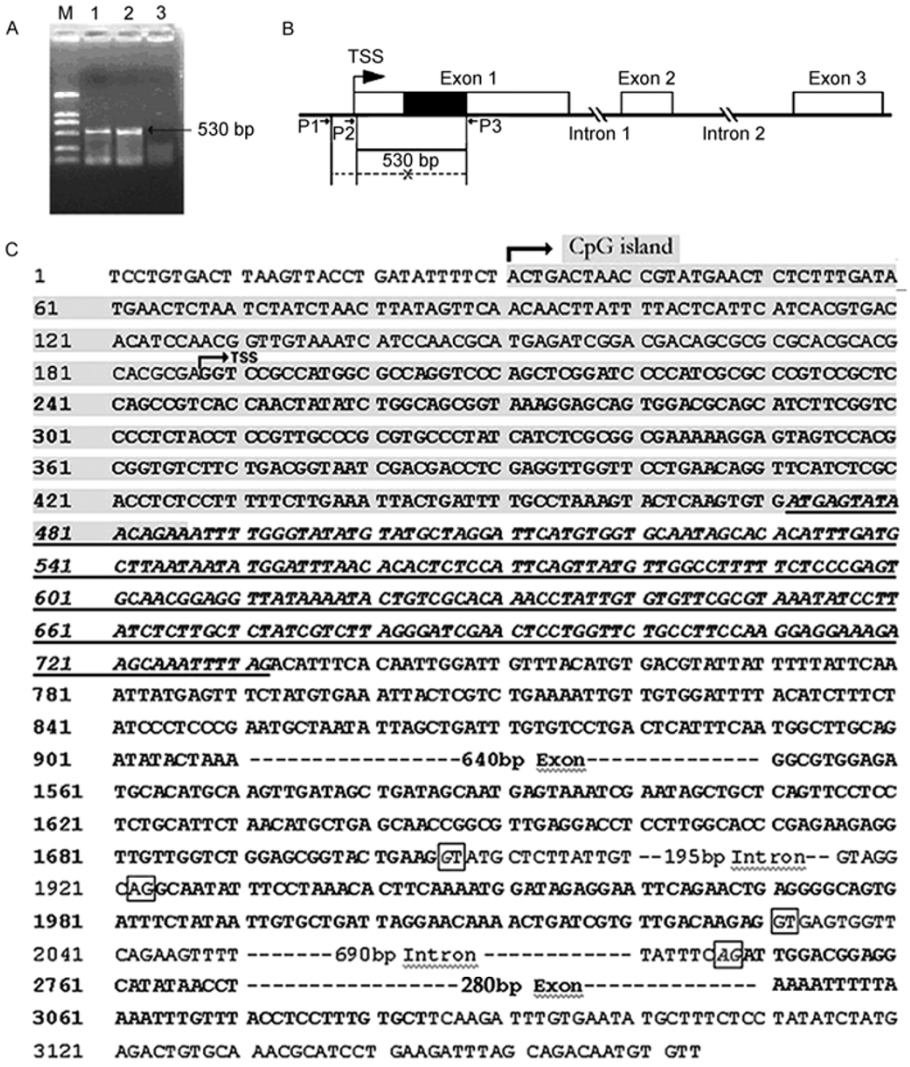

Figure 3 Analysis of *OsDPR* nucleotide sequence. A, Agarose gel electrophoresis analysis. Lane M, Marker D2000 (Tiangen Biotech, China); lanes 1 and 2, fragments amplified with primer set 2; lane 3, products amplified with primer set 1. Bent arrow indicates presence of targeted gene. B, *OsDPR* genomic sequence structure and primer design. Transcriptional start site (TSS) is indicated by bent arrow. ORF is located in first exon (black region). C, Nucleotide sequence of *OsDPR*. TSS at base pair 188 is shown by bent arrow. Sequence highlighted in gray is CpG island and includes 157 non-transcribed bp, TSS, a 284-bp 5′ UTR sequence, and 15 bp of coding region. Sequences in bold are exons of *OsDPR*; underlined sequence in first exon is the ORF. Boxes show boundaries of introns following GT-AG rule.

RNA using primer set 2 (p2 and p3), but there was no amplification product detected using primer set 1 (p1 and p3) (Figure 3A). The results confirmed those from the predictive bioinformatics analysis of the *OsDPR* sequence, and identified the TSS of *OsDPR* (Figure 3C). There is a CpG island within the promoter and the adjacent exon 1 of *OsDPR*. The boundaries of the introns strictly follow the GT-AG rule. The genomic sequence of *OsDPR* is shown in Figure 3C (GenBank accession number: DQ434846).

The OsDPR sequence was analyzed using bioinformatics tools. Using the TMHMM Server v.2.0, it was predicted that the OsDPR protein has a transmembrane domain near its C-terminus (Figure 4A). The SignalP-HMM (euk) prediction indicated that OsDPR might include a signal peptide approximately 19 amino acid residues long at its N-terminus (Figure 4B). The ExPASy PROSITE database suggested that there is a leucine zipper structure (L-x(6)-L-x(6)-L-x(6)-L) in OsDPR, located from amino acid residues 56 to 77 (Figure 4C). The leucine zipper pattern is present in many proteins that regulate gene expression, such as transcriptional factors/repressors and enhancer binding proteins, and it has been proposed to explain the function of some eukaryotic proteins regulating gene expression. The leucine zipper consists of a periodic repetition of leucine residues at every seventh position. The segments containing these periodic arrays of leucine residues seem to exist in an alpha-helical conformation. The leucine side chains extending from one alpha-helix interact with those from a similar

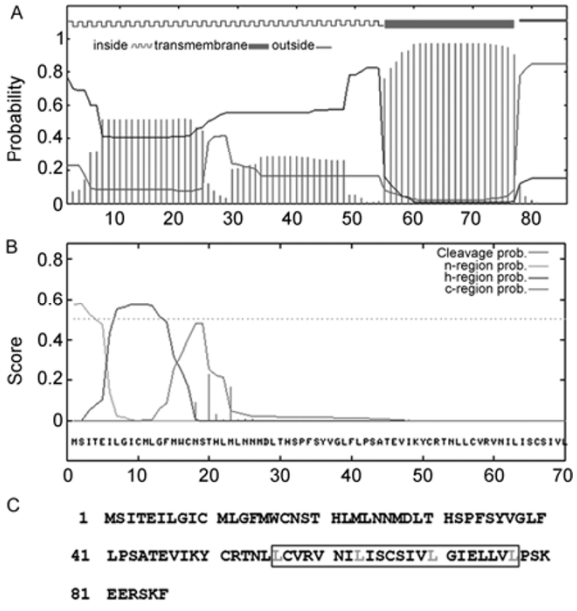

Figure 4 Analysis of OsDPR protein sequence. A, Transmembrane structure prediction result from TMHMM Server v.2.0. Abscissa represents amino acid sequence. B, Signal peptide prediction result from SignalP-HMM (euk). C, Leucine zipper pattern in OsDPR. OsDPR amino acid sequence is shown. Boxed sequence represents leucine zipper structure in which the repetitive leucine residues are shown in light grey.

alpha helix of a second polypeptide, facilitating dimerization to function (http://prosite.expasy.org/cgi-bin/prosite/nicedoc.pl?PS00029). This analysis raised the possibility that OsDPR may directly or indirectly interact with DNA sequences through dimerization. A search of public databases with OsDPR using BLASTp did not reveal any proteins with high levels of amino acid sequence similarity.

2.3 *OsDPR* suppresses growth of transgenic tobacco plants

To investigate the biological function of *OsDPR*, we constructed the stable plant expression vector pCAMBIA1302-*OsDPR*::*GFP* and produced transgenic tobacco plants. Wild-type and T3 transgenic tobacco progeny were grown under identical conditions and observed simultaneously. Phenotypic analysis indicated that the shoots of *OsDPR*-transgenic tobacco plants were smaller than those of wild-type plants (Figure 5A). The quantitative difference of seedling height between transgenic and wild-type plants is shown in Figure 5C. The roots of the transgenic tobacco plants were shorter than those of the wild-type plants under both iron-deficient and -sufficient conditions (Figure 5B). The quantitative comparison of root length between transgenic and wild-type plants is shown in Figure 5D. *OsDPR* expression resulted in reduced sizes of aerial parts and roots, indicating that *OsDPR* impedes the growth of tobacco plants.

The growth suppression caused by OsDPR was even stronger under iron-deficient conditions, because the roots of *OsDPR*-transgenic plants were even shorter than those of wild-type under iron deficiency (Figure 5D). Analysis of the OsDPR::GFP expression pattern, as detected by a GFP-Meter, showed that OsDPR::GFP was expressed in transformed plants at higher levels in iron-deficient conditions (Figure 5E). Thus, it can be presumed that the expression of OsDPR is also regulated by iron at the translational level. Transgenic tobacco plants accumulated more OsDPR under iron deficiency, resulting in a stronger suppression effect on root growth. As a novel gene, *OsDPR* was highly expressed under iron deficiency, and its protein translation

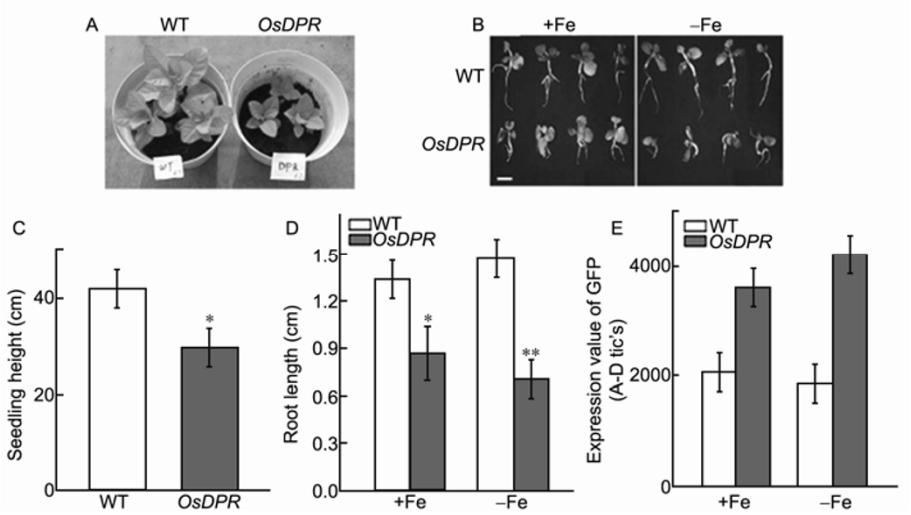

Figure 5 Comparison of phenotypes between wild-type and *OsDPR*-transgenic tobacco plants. A, Wild-type and *OsDPR*-transgenic tobacco plants on the 38th day after germination. B, Comparison of root length between transgenic and wild-type plants. Plants were cultivated on MS medium with (+Fe) or without (–Fe) iron. Scale bar, 5 mm. C, Quantitative comparison of seedling height between transgenic and wild-type tobacco plants after 78 days growth. D, Quantitative comparison of root length between transgenic and wild-type plants (*, $P<0.05$; **, $P<0.01$; $n=12$; three transgenic lines were evaluated). E, Detection of OsDPR::GFP expression in tobacco leaves. Plants were cultivated with (+Fe) or without (–Fe) iron. High detection values in wild-type plant are due to spontaneous fluorescence.

may also be regulated by iron.

Following successful germination, plant growth depends on a combination of two essential processes; cell division and cell expansion. These two processes play essential roles in the determination of plant size [13]. The growth-limiting effects of various kinds of stress have been related to their effects on the regulation of elongation and cell division [10]. As shown above, the *OsDPR*-transgenic plants exhibited reduced size of aerial parts, as well as shortened roots. To gain insight into how cell proliferation and/or cell expansion is regulated by *OsDPR*, we compared the morphology of root cells between the *OsDPR*-transgenic and wild-type tobacco plants by PI staining and laser scanning confocal microscopy. In the mature zone of the root tip, the cell size and shape were almost the same between wild-type and transgenic plants (Figure 6A). Furthermore, the cell length was not significantly different between the transgenic and wild-type plants (Figure 6B). These findings suggested that the root length of transgenic plants was limited by cell number, not cell size. This implied that a defect in cell proliferation, rather than cell expansion, was responsible for the dwarf phenotype of transgenic plants [14].

2.4 *OsDPR* slows cell proliferation in transgenic BY-2 cells

OsDPR-transgenic tobacco plants showed a clear growth defect, but had normal cell types, cell size, and cell shape. Therefore, we investigated whether *OsDPR* affected plant cell proliferation. We produced transformants of tobacco BY-2 cells expressing *OsDPR* (Figure 7B). Wild-type and *OsDPR*-transgenic BY-2 cells were cultured in identical NT medium and the fresh weight (Figure 7A) and A_{600} value (Figure 7C) of the two types of cells were measured every other day to determine the cell proliferation rate. Both the fresh weight and A_{600} value measurement indicated that the overall mass and cell number of *OsDPR*-transgenic BY-2 cells were lower than those of wild-type cells after the same period of culture. This indicated that the rate of cell production was significantly reduced in *OsDPR* transformants, and implied that *OsDPR* caused defects in normal cell division of BY-2 cells.

2.5 Down-regulation of *CyclinD2.1* in *OsDPR*-transgenic tobacco plants

In many cases, suppression of cell division activity is directly related to slower cell cycle progression. Since the rate of cell division was reduced by *OsDPR*, we anticipated that the transformants could have a defect in cell cycle progression. To investigate the role of *OsDPR* in the plant cell cycle, we examined the expression of a cell cycle checkpoint-related gene, *CyclinD2.1*, in *OsDPR*-transgenic and wild-type tobacco plants. There are essential regulatory checkpoints in the plant cell cycle. Cyclins and cytokines involved in the regulation of these checkpoints play an important role in cell division [15]. The D-type cyclins, which belong to the G1-phase cyclins, are required during the G1-to-S transition, which is a primary control point in the plant cell cycle [16]. Plant D-type cyclins respond to extracellular signals during the G1 phase [17] and are important sensors of cell cycle progress [2]. The modulation of plant growth rate is achieved by D-type cyclins [17].

The expression of *CyclinD2.1* in wild-type and T3 progeny of transgenic tobacco plants was detected by real-time PCR. Its expression in *OsDPR*-transgenic tobacco plants was significantly down-regulated compared with that in wild-type plants (Figure 8). This negative correlation suggested that *OsDPR* may participate in events controlling the cell cycle, so that cell division in *OsDPR* transformants was hindered, thereby reducing overall plant growth.

2.6 Nuclear localization of OsDPR

The results described above allowed us to identify the inhibition of plant growth caused by *OsDPR*. However, it was

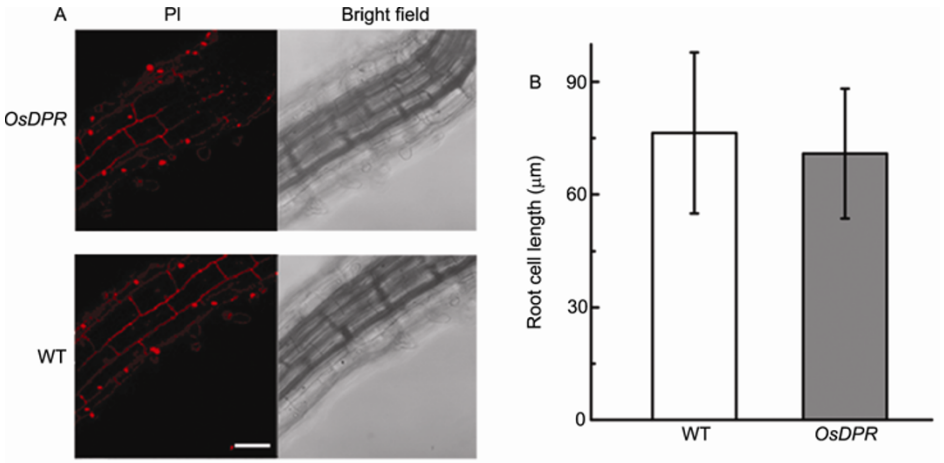

Figure 6 Root cells in wild-type and *OsDPR*-transgenic tobacco plants. A, Roots of transgenic and wild-type tobacco plants stained with PI solution. Scale bar, 50 μm. B, Quantitative comparison of cell length between transgenic and wild-type tobacco plants (120 mature cells from each sample were measured).

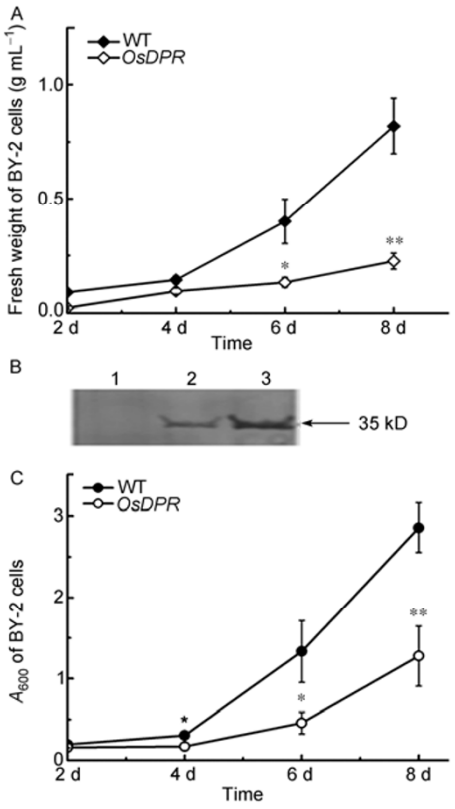

Figure 7 Growth rate of wild-type and *OsDPR*-transgenic BY-2 cells. A, Comparison of fresh weight between wild-type and transgenic BY-2 cells. A 1-mL aliquot of BY-2 cells was measured every other day. B, Western blotting of OsDPR::GFP in BY-2 cells. Extracts from wild-type BY-2 cells (lane 1) and extracts from transgenic cells (lanes 2 and 3); the 35-kD fusion protein OsDPR::GFP was detected with an anti-GFP antibody. C, Comparison of A_{600} value between wild-type and transgenic BY-2 cells. *, $P<0.05$; **, $P<0.01$, $n=3$.

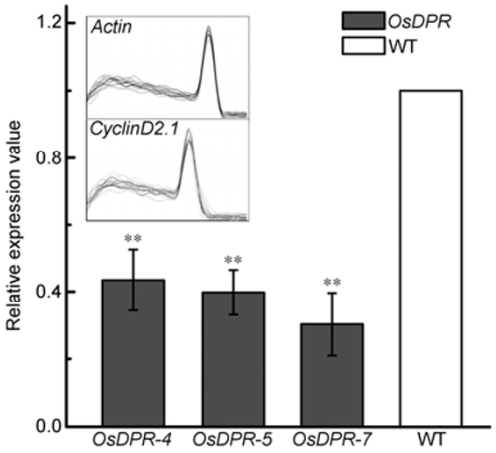

Figure 8 Real-time PCR of *CyclinD2.1* expression in tobacco plants. OsDPR-4, OsDPR-5, and OsDPR-7 are three different lines of transgenic tobacco plants. Wild-type tobacco (WT) served as the control. Inset pictures in the bar chart are melt curves of *Actin* and *CyclinD2.1*. **, $P<0.01$, $n=3$.

unclear how the phenotypes of the transformants were produced and how *OsDPR* down-regulated the expression of *CyclinD2.1*. Therefore, we investigated the cellular location of OsDPR to further analyze its function. To determine the subcellular localization of OsDPR, green fluorescent protein (GFP) fused with OsDPR (OsDPR::GFP) was transiently expressed in onion epidermal cells, and the GFP fluorescence was observed by laser scanning confocal microscopy. As shown in Figure 9, the fusion protein was clearly targeted to the nucleus, while the fluorescence was fairly uniform in the control cells expressing free GFP. No fluorescence was detected in untransformed onion epidermis (data not shown).

2.7 Suppressed phenotype in *OsDPR*-transgenic rice seedlings

To further clarify the effects of *OsDPR* expression on growth of rice plants, we transformed rice plants and obtained T0 transformants. The ectopic expression of *OsDPR::GFP* in transformants was detected by RT-PCR (Figure 10C). By comparing the phenotypes between transgenic and wild-type seedlings, we preliminarily confirmed that *OsDPR* inhibited rice growth. Under identical culture conditions, transgenic rice plants were clearly undersized (Figure 10A). This kind of phenotype was observed in more than 10 independent transgenic lines (Figure 10D). Figure 10B shows the quantitative comparison of seedling height between transgenic and non-transgenic plants. Compared with non-transgenic plants, the seedling height of transformants was significantly lower. These results indicated that *OsDPR* also restrained the growth of rice plants.

3 Discussion

The absorption and utilization of iron in plants is a complex and highly coordinated process. To cope with low iron sup-

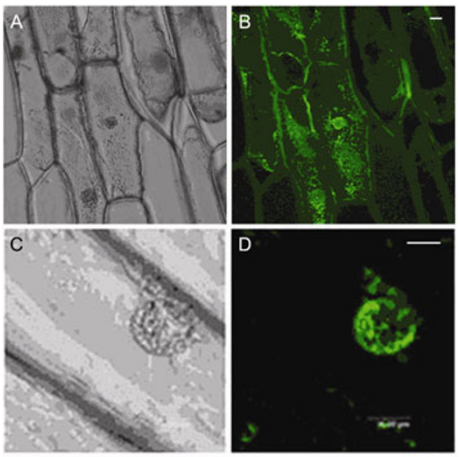

Figure 9 Subcellular localization of OsDPR::GFP fusion protein in onion epidermal cells. A and B, Light and fluorescent micrographs of onion epidermal cells with free GFP expression. C and D, Light and fluorescent micrographs of onion epidermal cells showing OsDPR::GFP localization pattern. Scale bar, 10 μm.

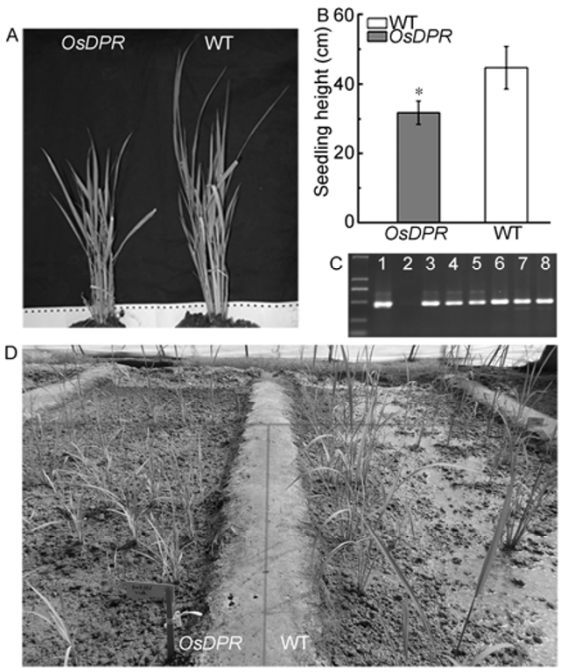

Figure 10 A, Comparison of phenotypes between *OsDPR*-transgenic and wild-type (WT) rice plants. B, Quantitative comparison of seedling height between transgenic and WT rice plants. *, $P<0.05$, $n=12$. C, Expression of *OsDPR::GFP* detected by RT-PCR. Marker D2000 (Tiangen Biotech, China) was used. Bands 465-bp long were amplified. Lane 1, positive control; lane 2, WT; lanes 3–8, six independent lines of transgenic rice plants. D, Overall comparison of growth between transgenic and WT rice plants in the field.

ply, plants initiate adaptive strategies and modulate the expressions of many related genes, which results in a series of physiological and morphological changes. In this study, we analyzed a gene, *OsDPR*, which is up-regulated under iron deficiency. The phenotype of the *OsDPR*-transgenic tobacco plants indicated that *OsDPR* restrained overall plant growth, including growth of roots and shoots. Plant growth is determined by two successive cellular processes; cell elongation and cell proliferation [2]. To understand the effect of *OsDPR* expression on plant cells, we observed the root cell morphology of transformed tobacco plants and compared proliferation rates of transgenic and wild-type BY-2 cells. The size and shape of cells was similar between transformants and wild-type plants, whereas *OsDPR* clearly slowed the proliferation rate of transgenic BY-2 cells. These results suggested that the inhibitory effects of *OsDPR* on plant growth were mainly related to cell division, not cell expansion. In addition, *OsDPR* down-regulated the transcription of the cell cycle-related gene *CyclinD2.1*. The D-type cyclins belong to the G1-phase cyclins and play an important role during the G1-to-S transition, which is a primary control point in the plant cell cycle and is essential for modulation of plant growth [16]. They respond to extracellular signals such as sucrose and hormones. The expression of *CyclinD* can be stimulated by these signals [17]. Research has shown that ectopic expression of *CyclinD2.1* in tobacco accelerates the rate of cell production by shortening the duration of the cell cycle [14]. In general, D-type cyclins are important sensors and also rate-limiting regulators of cell cycle progress [2]. Our study demonstrated that *OsDPR* down-regulates *CyclinD2.1* in tobacco plants and negatively regulates plant cell division. However, the molecular mechanisms underlying the suppression effects of *OsDPR* are largely unknown.

We determined the subcellular localization of OsDPR in onion epidermal cells. The fusion protein OsDPR::GFP was clearly targeted to the nucleus. The sequence of OsDPR includes a leucine zipper structure, which is a functional structure of many regulatory DNA-binding proteins such as transcription factors and enhancer binding proteins. Hence, the presence of this domain suggested that OsDPR might interact with DNA and play a role in the nucleus. The expression of *CyclinD2.1* was reduced by the *OsDPR*-transgene, so *OsDPR* may function as a transcriptional repressor in the nucleus. However, it was predicted by PSORT (http://psort.hgc.jp/) that OsDPR has no nuclear localization signal (NLS). Notably, some nuclear proteins, especially proteins with low molecular weight, do not include a typical NLS [18]. Further studies are required to clarify the functional mechanism of OsDPR in plant cells. According to the sequence analysis, OsDPR has a transmembrane domain near its C-terminus, but we did not detect membrane localization of OsDPR. It is possible that it is not a membrane protein, and that the transmembrane domain may be a hydrophobic part within the folding protein. There is a CpG island within the promoter and the adjacent exon 1 of *OsDPR*. Methylation of the CpG island might be involved in regulating the activity of the gene [19]. We searched public databases with OsDPR, but found no proteins with high levels of amino acid sequence similarity. Therefore, *OsDPR* is a novel gene that participates in regulating plant growth.

OsDPR is a rice gene induced by iron deficiency. Our results showed that it suppresses growth in both tobacco and rice plants. This suppressive effect may be a kind of adaptive response in plants under iron-deficient conditions. After years of evolution, plants have gradually acquired a variety of strategies to adapt to adverse environmental conditions. Under iron deficiency, some iron-related genes in plants, like *IRT1* and *FRO1*, are highly expressed to enhance the efficiency of iron uptake. There are also some changes in morphology, such as more abundant and longer root hairs, which expand the area for iron absorption. While actively improving the plant's ability to take up iron, plants might reduce iron use to keep growing with minimum nutrition consumption. The gene *OsDPR* is predicted to function in such an "economical" strategy. That is, when iron is insufficient, *OsDPR* slows the growth rate of plants, reducing the consumption of nutrients. This would enable the plant to survive with a low cost. Therefore, it is predicted that *OsDPR* plays a protective role in rice under iron deficiency

to some extent. However, further research is needed to determine the specific function and mechanism of *OsDPR* under iron deficiency.

*We gratefully acknowledge Prof. James O. Berry (*State University of New York, Buffalo*, USA) for critically reading the manuscript and providing suggestions to the paper. We thank Elsevier language services for revising the manuscript. This work was supported by the National Natural Science Foundation of China (Grant No. 30170552) and the Academic and Technical Development Key Project Foundation of Beijing Education Community (Grant No. KZ200710028013).*

1 Guerinot M L, Yi Y. Iron—nutritious, noxious, and not readily available. Plant Physiol, 1994, 104: 815–820
2 Jia L Q, Wu Z C, Hao X, *et al*. Identification of a novel mitochondrial protein, short postembryonic roots 1 (SPR1), involved in root development and iron homeostasis in *Oryza sativa*. New Phytol, 2011, 189: 843–855
3 Grotz N, Guerinot M L. Molecular aspects of Cu, Fe and Zn homeostasis in plants. BBA-Mol Cell Res, 2006, 1763: 595–608
4 Morrissey J, Baxter I R, Lee J H, *et al*. The ferroportin metal efflux proteins function in iron and cobalt homeostasis in *Arabidopsis*. Plant Cell, 2009, 21: 3326–3338
5 Ogo Y, Kobayashi T, Itai R N, *et al*. A novel NAC transcription factor, IDEF2, that recognizes the iron deficiency-responsive element 2 regulates the genes involved in iron homeostasis in plants. J Biol Chem, 2008, 283: 13407–13417
6 Walker E L, Connolly E L. Time to pump iron: iron-deficiency-signaling mechanisms of higher plants. Curr Opin Plant Biol, 2008, 11: 530–535
7 Eide D, Broderius M, Fett J, *et al*. A novel iron-regulated metal transporter from plants identified by functional expression in yeast. Proc Natl Acad Sci USA, 1996, 93: 5624–5628
8 Yang G, Ma F, Wang Y, *et al*. Vesicle-related OsSEC27P enhances H^+ secretion in the iron deficient transgenic tobacco root. Chin Sci Bull, 2010, 55: 3298–3304
9 Yin L P, Sun T, Huang Q N. Analysis of transcriptome and proteomics during Fe-deficiency stress in rice root and vesicle transport. Prog Nat Sci, 2004, 2: 522–527
10 Ding L, Jing H W, Qin B, *et al*. Regulation of cell division and growth in roots of *Lactuca sativa* L. seedlings by the ent-kaurene diterpenoid rabdosin B. J Chem Ecol, 2010, 36: 553–563
11 Laemmli U K. Cleavage of structural proteins during assembly of head of bacteriophage-T4. Nature, 1970, 227: 680–685
12 Towbin H, Staehelin T, Gordon J. Electrophoretic transfer of proteins from polyacrylamide gels to nitrocellulose sheets: procedure and some applications. Proc Natl Acad Sci USA, 1979, 76: 4350–4354
13 Dahan Y, Rosenfeld R, Zadiranov V, *et al*. A proposed conserved role for an avocado *fw2.2-like* gene as a negative regulator of fruit cell division. Planta, 2010, 232: 663–676
14 Hu Z B, Qin Z X, Wang M, *et al*. The *Arabidopsis* SMO2, a homologue of yeast TRM112, modulates progression of cell division during organ growth. Plant J, 2010, 61: 600–610
15 Gutierrez C, Ramirez-Parra E, Castellano M M, *et al*. G_1 to S transition: more than a cell cycle engine switch. Curr Opin Plant Biol, 2002, 5: 480–486
16 den Boer B G W, Murray J A H. Triggering the cell cycle in plants. Trends Cell Biol, 2000, 10: 245–250
17 Cockcroft C E, den Boer B G W, Sandra Healy J M, *et al*. CyclinD control of growth rate in plants. Nature, 2000, 405: 575–579
18 Wang X. Functional analysis of TaRAN1, a small GTP-binding protein during cell cycle and development in plant. Dissertation for Doctoral Degree. Beijing: Institute of Botany, Chinese Academy of Sciences, 2004
19 Balch C, Yan P, Craft T, *et al*. Antimitogenic and chemosensitizing effects of the methylation inhibitor zebularine in ovarian cancer. Mol Cancer Ther, 2005, 4: 1505–1514